Chapter 5

Apodization of Fiber Gratings

Light + Light does not always give more light,
but may in certain circumstances give darkness.
—Max Born

Interestingly enough, *apodization*[1] is a word often encountered in filter design; a word that flows easily off the tongue. Yet many readers are not aware of the exact meaning of the term. Etymologically, the word has its roots firmly in Greek, *a podos*, meaning "private-foot," in other words, hidden foot — footless. Curiously, any of the approximately 150 species of the amphibian order *Gymnophiona*, known as caecilian, were formerly known as *Apoda*. They are burrowing or swimming, secretive animals, without limbs but with an elongate body length between 100 and 1500 mm, occurring in the Western Hemisphere [1]. Not unlike fiber gratings. . .

So what does the word mean when applied to fiber grating filter design? Fiber gratings are not infinite in length, so they have a beginning and an end. Thus, they begin abruptly and end abruptly. The Fourier transform of such a "rectangular" function immediately yields the well-known *sinc* function, with its associated side-lobe structure apparent in the reflection spectrum. The transform of a Gaussian function, for example, is also a Gaussian, with no side lobes. A grating with a similar

[1]Etymology: Greek. *a*, private, *podos*, a foot. Source: *Chambers 20th Century Dictionary.*

refractive modulation amplitude profile diminishes the side lobes substantially. The suppression of the side lobes in the reflection spectrum by gradually increasing the coupling coefficient with penetration into, as well as gradually decreasing on exiting from, the grating is called apodization. Hill and Matsuhara [2,3] showed that apodization of a periodic waveguide structure suppresses the side lobes. However, simply changing the refractive index modulation amplitude changes local Bragg wavelength as well, forming a distributed Fabry–Perot interferometer [4], which causes structure to appear on the blue side of the reflection spectrum of the grating, although side-lobe amplitudes are reduced [5]. To avoid this complication, the key is to *maintain* an unchanging average refractive index throughout the length of the grating while gradually altering the refractive index modulation amplitude.

The alternative approach for generating a reflection spectrum that has a constant reflectivity over a certain band and zero outside of it is to write a sin x/x refractive index modulation envelope. From the Fourier transform analogy, it is apparent that the grating reflection spectrum will be a "top-hat" function. The problem, however, is to incorporate the grating in such a way that the fringes have the appropriate phase relationship on either side of the zeroes of the *sinc* function. Since the induced refractive index change is proportional to the square of the electric field amplitude (intensity), it is always positive. The phase change can be physically incorporated either by including a $\lambda/4$ dead zone in which no grating exists at each zero or by changing the phase of the grating abruptly, for example in a phase mask [6] or slowly over the length of the section [7]. Strictly speaking, the Fourier transform analogy is only applicable to weak gratings, as mentioned in Chapter 4. However, the principle of using the space–frequency transform does allow the techniques to be used for the design of gratings.

The beneficial effects of apodization are not manifest only in the smoothness of the reflection spectrum, but also in the dispersion characteristics. There are many techniques, as there are appropriate profile functions (*shading*) for the refractive index modulation amplitude to achieve the end result. However, they all rely on a single principle: keeping the *sum* of the dc index change and the amplitude of the refractive index modulation constant throughout the grating. In the following section, several of these techniques and types of "shading" functions used for apodization are reviewed.

5.1 Apodization shading functions

In filter and information theory, there are well-established functions for capturing a signal with a given bandwidth for the required signal to noise ratio [8]. Generally, these are known as Hamming and Hanning functions. The distinguishing feature between the two is whether or not the function forces the filter parameter to zero at infinite "detuning." For example, if the window function profiling the refractive index modulation amplitude reduces it to zero at either end of the grating, it is known as a Hanning, and otherwise a Hamming function. There are various types of functions, each of which results in a compromise between roll-off of the filter and the useable bandwidth. For the numerical analysis commonly used for the computation of the response and also to define the functions for apodization and chirp, it is convenient to define the grating function as

$$\Delta n(z) = \frac{\Delta n_{\max}}{2} f_A(z) f_g(z) + \varepsilon \frac{\Delta n_{\max}}{2}, \tag{5.1.1}$$

where the maximum ac index change is indicated by the subscripted variable n, $f_A(z)$ and $f_g(z)$ are the apodization envelope and periodic refractive index modulation functions, and $0 \leq \varepsilon \leq 2$ is a parameter that controls the level of the background, dc index change. In general the function, $f_g(z)$ includes chirp as

$$f_g(z) = \cos\left(\frac{2\pi z}{\Lambda_0 + \mathbf{F_g}\left(\left[TRUNC\left(\frac{N_g z}{L}\right)\delta\Lambda\right]^m\right)}\right), \tag{5.1.2}$$

where Λ_0 is the period at the start of the of the grating, and $\mathbf{F_g}$ is a function that describes the spatial variation of the grating period with a power dependence m and chirp step $\delta\Lambda = \Delta\Lambda/N_g$ (where $\Delta\Lambda$ is the total chirp of the grating). The grating is composed of N_g discrete sections. The apodisation factor $f_A(z)$ is described by a number of commonly used functions $\mathbf{F_g}(\theta)$ and has an argument of the form

$$\theta = 2\pi\left[\text{Trunc}\left(\frac{N_A z}{\Lambda_A}\right) + \phi_A\right] \tag{5.1.3}$$

where N_A is the number of sections in the entire grating, Λ_A is the apodisation envelope period, and ϕ_A is a starting phase.

Commonly used functions are as follows:

1. Raised cosine: $$f_A(z) = \cos^n(\theta) \tag{5.1.4}$$

2. Gaussian: $$f_A(z) = \exp\left[-G\left(\frac{\theta}{2\pi}\right)^2\right] \tag{5.1.5}$$

3. Tanh: $$f_A(z) = 1 + \tanh\left[T\left(1 - 2\left|\frac{\theta}{\pi}\right|^{\alpha}\right)\right], \tag{5.1.6}$$

where the phase offset has been set to zero.

4. Blackman: $$f_A(z) = \frac{1 + (1 + B)\cos(\theta) + B\cos(2\theta)}{2 + 2B} \tag{5.1.6}$$

5. Sinc: $$f_A(z) = \sin^A\left[0.5\left(\frac{\theta}{\pi}\right)^B\right] \tag{5.1.7}$$

6. Cauchy: $$f_A(z) = \frac{1 - (\theta/\pi)^2}{1 - (C\theta/\pi)^2}. \tag{5.1.8}$$

Three of these apodisation functions, the Tanh, raised cosine, and cosine, are shown in Fig. 5.1 for a grating that has a full chirped bandwidth of 0.8nm and is 100 mm long. The reflectivity has been adjusted to be ~90%, with a peak-to-peak refractive index modulation of 8×10^{-5}.

The beneficial effect of apodization is in the removal of a strong ripple in the group delay. The corresponding effect on the relative group delay as

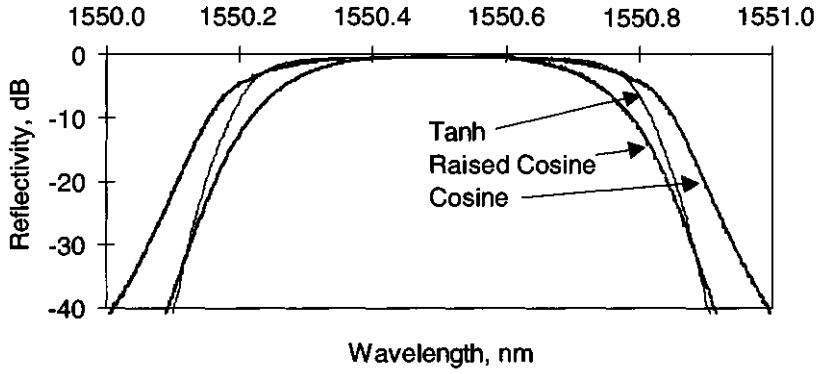

Figure 5.1: The reflectivity spectrum of a 100-mm-long, 0.8-nm bandwidth chirped grating, designed to compensate the dispersion of 80 km of standard fiber, with tanh, $\cos^2$, and cosine apodization envelopes.

a function of wavelength, of the apodization profiles shown in Fig 5.1 is demonstrated in Fig. 5.2. The role of the ripple is considered in Chapter 7.

5.2 Basic principles and methodology

In the discussion that follows, the aim of the exercise is to ensure that the effective index of the grating remains constant, even though the coupling constant becomes a slowly varying function of grating length. The approaches taken to solve this problem are either optical or mechanical, i.e., to program the variation in the coupling constant of the grating at a point, or a combination of both. Optical methods include the use of coherence properties of the UV source and the stamping of short overlapping gratings to build a composite. Mechanical techniques rely of physically blurring out the fringes in a controlled manner, by physically stretching the fiber or shaking it. Finally, a combination of the two may also be used to make complex gratings. Also discussed in the following sections is a specific example of the "top-hat" grating, one with the ideal filter characteristics: a reflectivity that is constant in-band and zero out-of-band, being another form of apodization. This type of a function is highly desirable for a vast number of applications in telecommunications but is restricted to unchirped gratings. Chirping apodizes a uniform refractive index modulation grating as well and may be used for broadband reflectors. Chirped

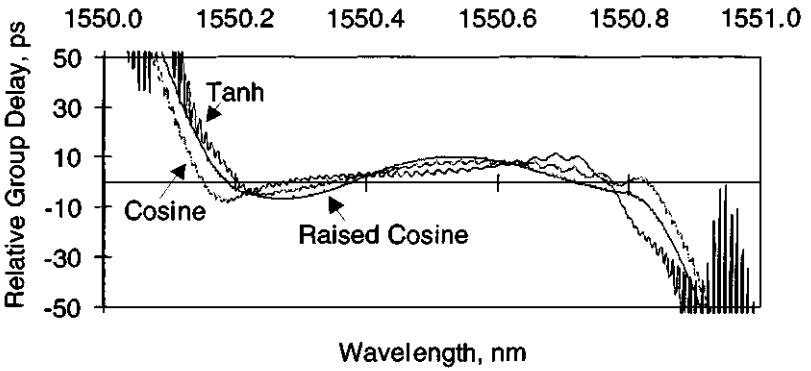

Figure 5.2: The effect on the relative group delay of the apodization profiles used for Fig. 5.1. Although the tanh profile has a flatter characteristic, it also has more residual ripple.

gratings have an associated dispersion that may not be desirable for high-speed applications, unless the grating length is much less than the length of the pulse in the fiber, in which case the grating becomes a point reflector.

5.2.1 Self-apodization

Figure 5.3 shows the region of overlap of two monochromatic UV beams with intensities I_1 and I_2 with a mutual angle θ_m. The intensity $I(z)$ at any point z along the z-axis varies according to the phase-difference between the two beams and can be shown to be

$$I(z) = I_1 + I_2 + 2\sqrt{I_1 I_2}\cos\left[\frac{2\pi}{\lambda_{UV}}\sin\left(\frac{\theta_m}{2}\right)(L_g - 2z)\right], \quad (5.2.1)$$

where the term in brackets is the mutual phase difference between the two beams, and L_g is the length of the overlap, where a fiber grating can form. The function is periodically modulated, and its visibility is

$$v = \frac{I_{\max} - I_{\min}}{I_{\max} + I_{\min}}, \quad (5.2.2)$$

determined by the maximum and minimum intensities in the fringes. The visibility is unity along the entire length L_g only if the radiation is monochromatic *and* the amplitudes of the two beams are identical.

If the UV radiation is composed of two monochromatic frequencies, then the interference pattern is the sum of Eq. (5.2.1) for the frequencies

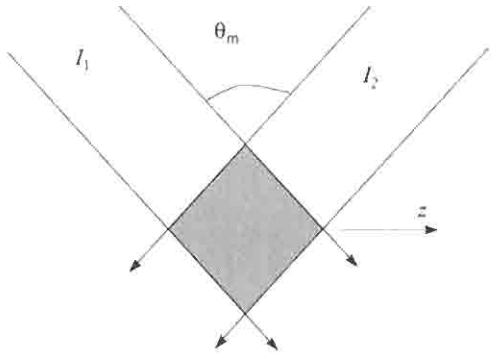

Figure 5.3: The overlap of two beams in the z direction.

present in the source. This leads to a situation in which the visibility of the fringes becomes a function of z. The two sets of fringes with different periods according to Eq. (5.2.1), one for each frequency. For this simple case, the form of the visibility function is simply the "beat" envelope, with the fringe visibility vanishing at positions $\pm z$ from the center of the overlap region at which the fringes from one frequency get out of phase with those from the other. The envelope is described by the function

$$I(z) \cong 2 + 2\cos\left(\frac{2\pi Z_g}{\lambda_{UV}}\right)\cos\left(\frac{2\pi Z_g}{\lambda_{UV}}\left(\frac{\Delta\lambda}{\lambda_{UV}}\right)\right), \tag{5.2.3}$$

where

$$Z_g = \sin\left(\frac{\theta_m}{2}\right)(L_g - 2z). \tag{5.2.4}$$

In Eq. (5.2.3), the interference term has been retained from Eq. (5.2.1), and equal, unity UV intensity of the interfering beams has been assumed. The first term on the RHS is identical to that of Eq. (5.2.1). However, notice that the fringes are now modulated by a slowly varying function with the argument dependent on $\Delta\lambda$, the difference in the wavelength between the two frequencies of the source.

For the general case of a source with a Gaussian spectral content, the visibility function becomes an integral over the bandwidth. The points at which the visibility vanishes are determined by the bandwidth of the source. For a particular length of the illuminated region, the fringes vanish at the edges, replaced by constant UV illumination. For a uniform intensity beam profile of the laser beam, the fringes are *self-apodizing* [9]. With the induced index change being proportional to the fringe amplitude, the interference pattern is written into a fiber core when exposed at this position. Figure 5.4 shows the fringes including the self-apodizing envelope for a 100-micron-long grating. The fringe period has been chosen for illustration purposes only. For real laser systems, it is possible to apodize grating lengths approaching ~50 mm [9].

The principle of apodisation described above is based on the moiré effect. Apodization occurs in the presence of two gratings of different periods, without affecting the total UV dose. The envelope of such a moiré grating is a cosine function, and to alter it, for example, to a Gaussian, a laser with the appropriate spectral shape may be used. This could be a broadband frequency-doubled dye laser source.

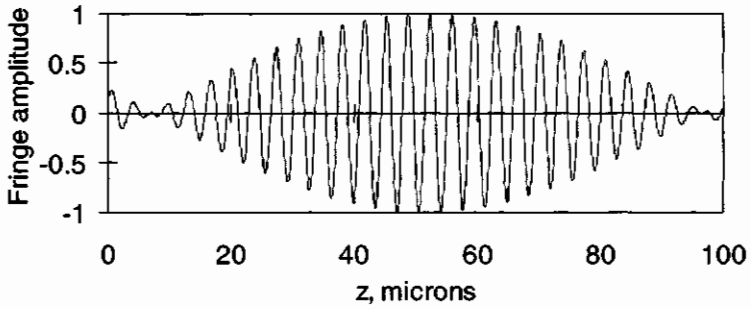

Figure 5.4: The self-apodized fringe profile of a two-wavelength source. The parameters have been chosen for illustration purposes only [9]. The grating length must be chosen to exactly match a single period of the envelope. Since this process has not modified the beam intensity profile, the change induced in the effective index of the mode by the UV dose is the same all along the fiber.

There are other methods of generating moiré[2] patterns for apodization. An optical wedge placed in the path of one of the beams of the UV interferometer will change the Bragg wavelength of the grating being written. Removal changes the Bragg wavelength; if the wedge angle is chosen such that the wavelength difference between the two Bragg periods is exactly *one* period more or less over the length of the grating, then apodization will occur. In this case, the difference in the Bragg grating period is given by

$$\Delta\lambda \approx \frac{\Lambda_{Bragg}^2}{L_g} . \tag{5.2.5}$$

The wedge required for this purpose must impart a π phase change from one end of the grating to the other. Thus, for ~10-mm-long gratings, a wedge angle of the order of 5′ to 10′ of arc is required at a Bragg wavelength of ~1550 nm [9].

Now that the principles have been set out whereby apodization can be performed without altering the intensity of illumination across the length of the grating, other practical implementations are discussed in the following sections.

[2]Etymology: *Fr.*, watered silk; referring to pattern formed on it.

5.2.2 The amplitude mask

Amplitude shading of the intensity profile of the interference pattern (for example, the natural Gaussian profile of a laser beam) helps reduce the side lobes in the reflection spectrum. However, a symmetric "chirp" is also incorporated in the grating such that the blue part of the reflection spectrum acquires an ugly structure (see Chapter 9). This is not good for systems in which many such filters may be required to isolate tightly packed channels. Clearly, simple amplitude shading is not in itself useful for apodization. However, amplitude masks may be used in conjunction with corrective measures to alter the waveguide parameters to result in a constant effective index of the mode. The method developed to apodize gratings relies on a double exposure: the first to precondition the fiber with an amplitude mask, followed by the inscription of the grating again with another amplitude mask in conjunction with a phase mask [10]. The dose in the preconditioning exposure is adjusted to allow for the inscription of the grating with a symmetric fringe intensity profile.

In Fig. 5.5 the preconditioning and grating illumination profiles are shown along with the period-averaged UV intensity. The envelopes of the precondition and the fringes are orthogonal functions. The result of apodization on the reflection spectrum due to the double exposure is

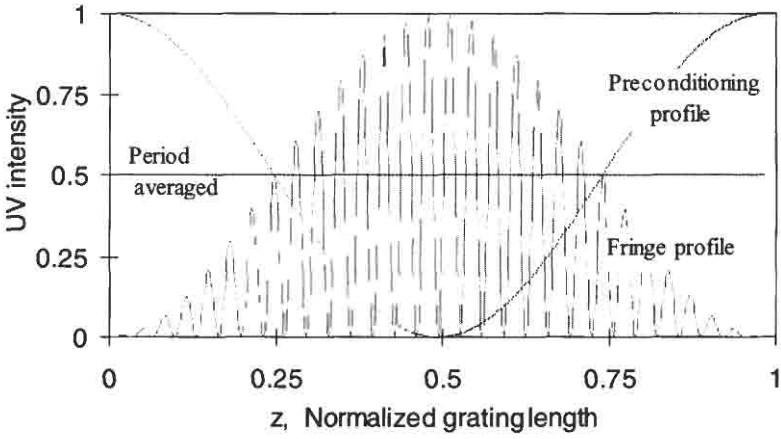

Figure 5.5: The preconditioning UV intensity shaped by the amplitude mask, the fringe profile, and the period-averaged UV intensity is shown. Since the average UV intensity is constant as a function of position, so is the effective index.

shown in Fig. 5.6. A clear reduction of ~20 dB in the side lobes is apparent over the unapodized grating of the same strength, with a reflectivity of 90% and a FWHM bandwidth of 0.24 nm. At ±0.4 nm away from the peak of the reflection, the reflection is less than −40 dB relative to the peak. The fiber used for fabricating the grating was standard Corning SMF-28, which was hydrogen loaded prior to processing. The refractive index modulation profile chosen for this grating was a $\cos^2$ function, which was closely reproduced in the resultant grating. This type of a filter is difficult to fabricate using any other technology and demonstrates the immense signal discrimination available with properly fabricated fiber gratings.

While the process of double exposure can produce excellent results as already demonstrated, it requires a careful study of each and every type of fiber to be used for the fabrication of apodized gratings. The final result depends not only on the photosensitivity and composition of the

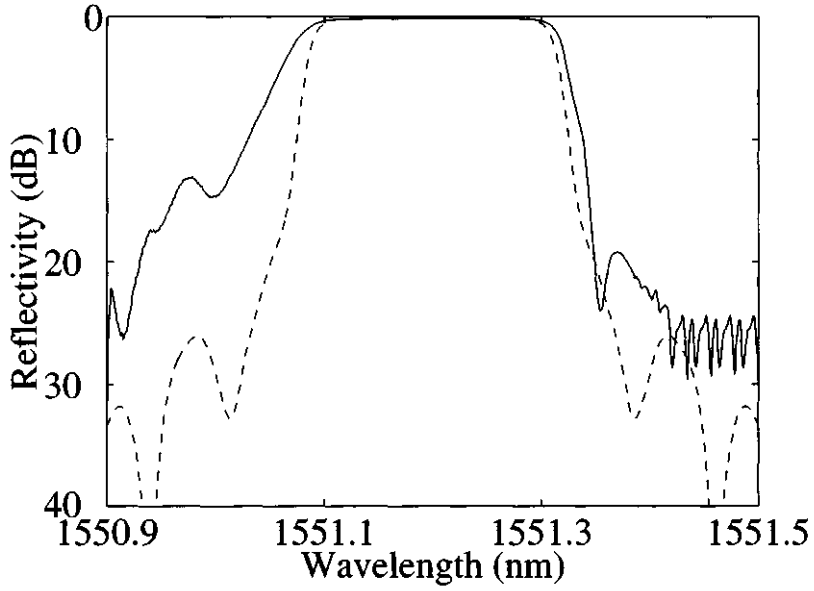

Figure 5.6: The reflection spectrum of an unapodized grating and a $\cos^2$ fringe envelope profile apodised grating written by the double exposure method. The grating length is 10 mm (from: Malo B., Thériault S., Johnson D. C., Bilodeau F., Albert J., and Hill K. O., "Apodised in-fibre Bragg grating reflectors photoimprinted using a phase mask," *Electron. Lett.* **31**(3), 223–225, 1995.) © *IEE* 1995.

fiber, but also on the type of exposure, whether hydrogen loaded or not, use of a pulsed or CW source, as well as the wavelength of the UV radiation. A further complication may occur due to the effects of "incubated" grating formation [11], in which nonlinear growth of a grating occurs. It is therefore expected that other methods may be easier to use routinely, requiring less processing.

5.2.3 The variable diffraction efficiency phase mask

A phase mask with a variable diffraction efficiency has been used for the fabrication of apodized gratings [12]. There are two methods of fabricating such a mask. The diffraction efficiency into the +1 and −1 orders is maximized for a 1:1 mark–space ratio of the grating and the zero order minimized for a specific groove depth (see Chapter 3). Therefore, there are two degrees of freedom to alter the diffraction efficiency. The mark–space ratio of the grating etched in the phase mask or the groove depth may be varied. In the technique reported, a variable diffraction efficiency phase mask, was fabricated by direct exposure of a silica plate to an ion beam of silicon. In this direct write method the ion beam was focused to a spot diameter of 100 nm and scanned across the plate to delineate the grooves. Wet etching in a 1-mol% solution of hydrofluoric acid in water was used to develop the mask. It was demonstrated that the etching rate is dose dependent. Groove widths between 100 and 550 nm and depths from 7.5 to 300nm could be achieved by varying the ion dose from 0.5 to 4×10^{14} ions/cm^2. The etch rate is faster for regions exposed to higher doses. The diffraction efficiency into the ± 1 and 0 orders was measured as a function of the dose; the diffracted orders were shown to be a linear function up to a dose of 2.25×10^{14} ions/cm^2. Thus, a variable diffraction efficiency phase mask was fabricated, using a Gaussian profile dose of $(2.25 \times 10^{14}$ ions/cm$^2)$ $\exp(-x^2/(0.420)^2)$, where x is measured in mm from the center of the 1-mm-long grating, with a period of 1.075 μm. One of the difficulties of fabricating such a grating is the stepped movement of the ion beam. As a result, the Gaussian phase mask profile can only be approximated, and altering the dose in 40 dose steps did this.

Subsequently, apodized gratings were imprinted in standard telecommunications hydrogen loaded fiber and shown to have reduced the first set of side lobes by approximately 14 dBs for a 10% reflectivity grating. These results are not as good as those from the double exposure method (see Section 5.2.2) in which a reduction in the side lobes of 20 dB was

achieved for a reflectivity 10× greater. It is anticipated that the fabrication of longer gratings is not only likely to be difficult owing to uniformity of the grating but also very expensive and time-consuming.

Phase masks fabricated with stepped sections have been demonstrated [13]. However, one of the problems with e-beam fabrication of phase masks is the step size, which can be programmed to allow a variable mark–space ratio of the grooves. An alternative to this approach is to write a moiré grating on the photoresist of the phase mask plate. Writing two gratings of different wavelengths so that at the edges, the two patterns are exactly half a period out of phase as shown in Section 5.2.1 easily does this. The dose delivered by the e-beam for each overlaid grating is half that required for the resist to be fixed. With two exposures, the correct dose is delivered [14] and on developing the mask, the moiré grating is revealed [15]. In this phase mask, the diffraction efficiency varies continuously along its length, and it is possible to fabricate phase masks for long gratings. While it is attractive and convenient to replicate apodized gratings directly using apodized phase masks, there are issues that need to be addressed, which are definite drawbacks in the fabrication and use of such a mask. The feature size of the mask near the edges of the grating becomes infinitesimal, and as a result, the features have no strength. Nor is there any guarantee that they will survive the phase mask fabrication process in a repeatable fashion. The fragility of such a phase mask makes it impossible to handle. It is likely to be damaged easily, either optically or mechanically, during the process of fiber grating replication. There is also the additional problem of the removal of contamination from such a fragile phase mask. The better option for an apodized phase mask is to alter the *etch depth* while keeping the mark–space ratio constant. This ensures the strength and eases handling and cleaning processes.

The next section explores two techniques based on the application of a combination of optical and mechanical methods. Both are highly flexible and capable of produce a variety of gratings, apart from simple apodization.

5.2.4 Multiple printing of in-fiber gratings applied to apodization

The multiple printing in fiber (MPF) method has been discussed in Chapter 3. In this section, the particular attributes and requirements for the fabrication of (a) apodised gratings and (b) top-hat reflection gratings is

discussed. The principle of this method is to write short (4-mm) gratings that are overlapped, so that at each printing only a few new periods are printed [16]. This is possible with a pulsed UV laser system but requires extreme precision in positioning the fiber. To overcome this problem, the fiber is supported over the entire length of the grating to be fabricated in a long glass vee-groove. The vee-groove is fabricated using two pieces of glass assembled together with a small gap at the apex of the vee. This allows a vacuum system to be used to hold the fiber precisely in position as it is translated. Figure 3.21 shows the overall fabrication equipment. Other important issues are the smoothness of the fiber translation system and the precise timing of the laser pulse. The former problem is overcome by translating the fiber *continuously* at a constant speed on an air bearing, during fabrication, using a linear motor capable of long translation (500 mm). The location of a point on the fiber carriage is measured continuously by an interferometer, which is modulated by a Pockels cell. This tracking interferometer has a resolution of ~0.3 nm over the translation distance. Part of the tracking signal is fed back to maintain a constant speed and to compensate for vibrations. The position of the interferometer is fixed, and the fiber is translated across the fringes, both backward and forward. The process is entirely controlled by a computer, which is programmed to generate a particular function in the firing sequence of the laser, movement direction, and speed of translation.

The schematic of the printing is shown in Figure 5.7. Overlapping fringes are shown in a sequence. The center shows the first printing of a grating; the bottom shows the position of the second printing relative to the first arranged to arrive just ahead of a fringe maximum already printed by a distance $+\delta$, and the top is the position of the third printing, which arrives immediately after the second pulse to write on top of the same fringe maximum but delayed by a distance $-\delta$. Also shown is the fringe in the fiber core at the third pulse, being a combination of the fringes due to the second and the third pulses only. As can be seen, the fringe spreads symmetrically around the original maximum. By altering the sequence of pulses, the fringes can be filled in so that the grating gradually disappears toward the edges.

Using this method, unapodized gratings with a FWHM bandwidth of 4.6 pm (L_g = 200 mm) and apodised gratings with a bandwidth of 27 pm (L_g = 50 mm) have been demonstrated [17], both close to theoretically predicted values for low-reflectivity gratings (2–3%). The method naturally allows any type of apodization to be programmed in.

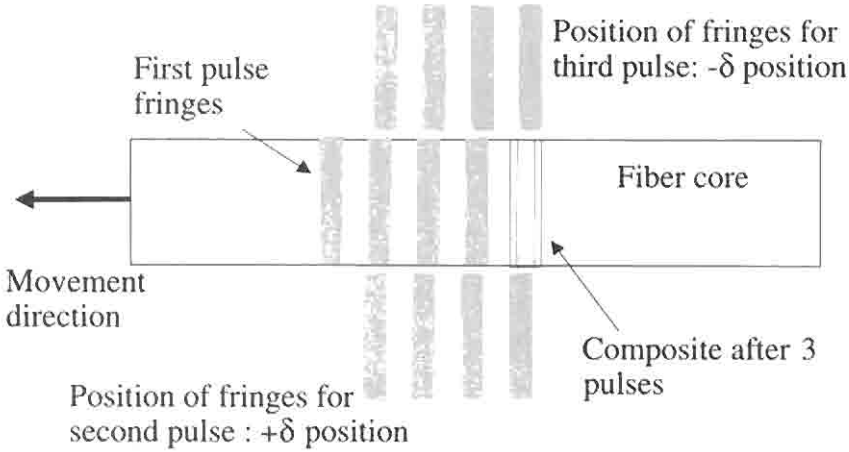

Figure 5.7: The sequence of pulses is staggered so that a fringe is spread symmetrically around the mean position of the fringe already printed in the first printing.

There are some points that need to be considered in the use of this method. The minimum step size determines how smoothly the grating can be apodized. The step size is of the order of 0.01 mm, so that typically in a grating length of 100 mm, full symmetric apodization can be achieved with a maximum of ~10,000 steps, which is more than adequate for a smooth profile. These parameters are discussed in Section 5.3.

This technique has been applied to the fabrication of apodized chirped gratings as well. In this case, not only does the mark–space ratio have to be changed but also the period.

5.2.5 Position-weighted fabrication of top-hat reflection gratings

The MPF method is suited to writing gratings with a "top-hat" (TH) reflection spectrum, shown in Fig. 5.8, along with the spatial profile of the refractive index modulation of the grating required for these characteristics (Fig. 5.9). For a perfect TH, an infinite number of cycles of a *rect* or *sinc* function are needed. This is not possible for practical gratings, since the continuous *sinc* function can only be approximated in a discrete number of steps. This task is demanding in any case, but a good approxi-

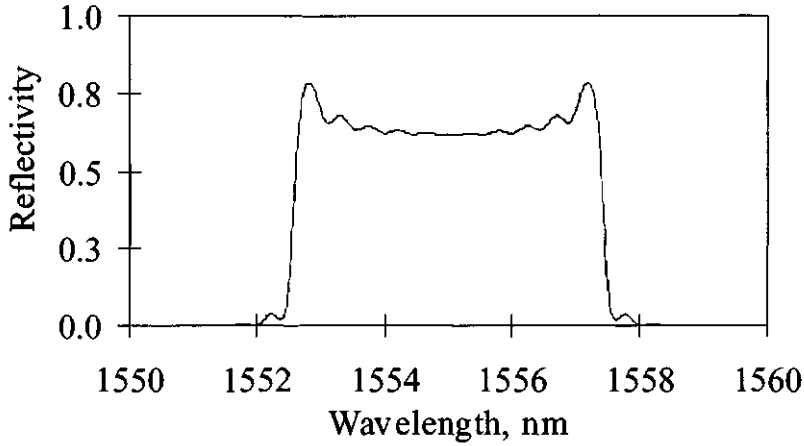

Figure 5.8: Simulated reflection spectrum of a *sinc* function approximated by including 22 zeroes for a grating 4 mm long. The peak-to-peak index difference is 6×10^{-3}, and the grating has 1000 sections. These gratings demand better step resolution than is possible with the MPF scheme.

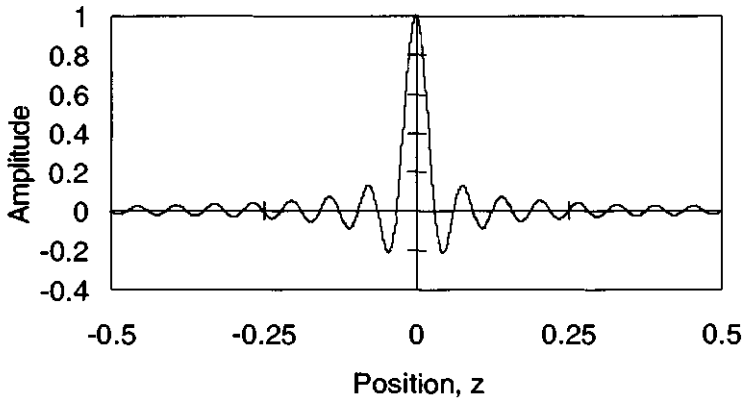

Figure 5.9: The refractive index modulation profile showing 31 zeroes along the length of the grating. Figure 5.8 shows a top-hat reflection spectrum for a grating with 22 zeroes. The modulation amplitude must have positive and negative components in order to faithfully reproduce a top-hat spectrum. Truncation leads to a limiting out-of band rejection of ~ -20 dB.

mation is possible with a few cycles. In order to invert the phase between the sections, additional UV exposure is given to induce a $\lambda/2$ phase shift.

The MPF scheme caters for both the changes in the amplitude of the refractive index modulation and the phase change. For the former, overlaid subgratings with the appropriate phase step between each printing reduce the fundamental component of the amplitude of the refractive index modulation. By the same technique, a phase change of π can also be introduced by shifting the fiber by the appropriate distance prior to the printing of the next subgrating. This method allows a very high degree of flexibility in the fabrication of gratings [17].

The positions for the phase steps are shown in the refractive index amplitude profile in Fig. 5.10. In trying to reproduce faithfully the TH function by an approximate method, two difficulties are encountered. The truncated *sinc* function throws up additional frequency components, which create out-of-band reflections, since exact cancellation of the phases is no longer possible. Secondly, the approximate envelope of each period of the *sinc* function introduces additional phase shifts, which has a deleterious effect in the out-of-band spectrum. Typically, the background reflection remains just below 20 dB over a wide out-of-band frequency spectrum. A measured response of a 100-mm-long truncated *sinc*, TH grating is

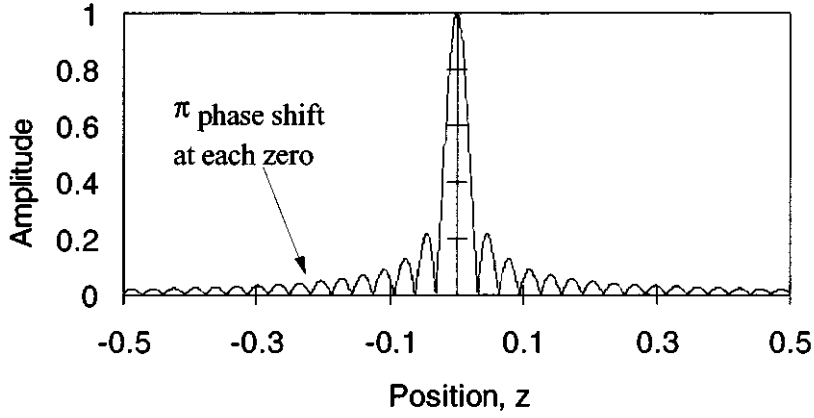

Figure 5.10: The actual refractive index modulation amplitude written in the fiber. In order to introduce the change in the sign of the modulation, a phase change can be placed at the zero.

shown in Fig. 5.11. The achieved results are close to those of the simulation. The bandwidth is ~20 GHz, with a roll-off of 4 dB/GHz at the band edges, and a peak in band reflectivity of ~55%. The out-of-band rejection was not ideal, being only 16 dB below the in-band reflection, but can be improved by making the grating longer.

Combining other shading functions with the *sinc* profile can reduce the out-of-band reflection to below 50 dB [19]. Although it is possible to fabricate such gratings with the MPF method, the steep edges of the TH spectrum are degraded, and it is not clear whether or not a strong grating apodized using another simple function may be a better option.

5.2.6 The moving fiber/phase mask technique

The MPF technique relies on the fiber being translated across an interference fringe pattern in synchronism with the arrival of the UV writing pulse. With the use of a CW beam, this is not possible since the grating would be washed out. This is exactly the principle of the moving fiber/phase mask (MPM) writing scheme: The fiber is moved along with the phase mask in front of a stationary UV beam, or with the UV beam scanned across a fixed phase mask, with the fiber moving slowly relative to phase mask. Figure 5.12 demonstrates the principle of scanning the UV beam across the phase mask. The fiber is mounted on a holder that can be moved in its entirety (as with the MPF method) but using a

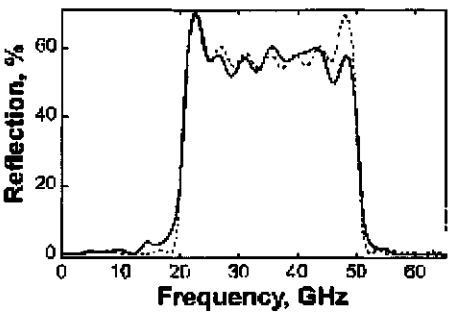

Figure 5.11: The reflection spectrum of a 100-mm-long TH grating. The grating is a result of a truncated *sinc* function made with the MPF method (from: Storøy H., Engan H. E., Sahlgren B., and Stubbe R., "Position weighting of fiber Bragg gratings for bandpass filtering," *Opt. Lett.* **22**(11), 784–786, June 1, 1997.)

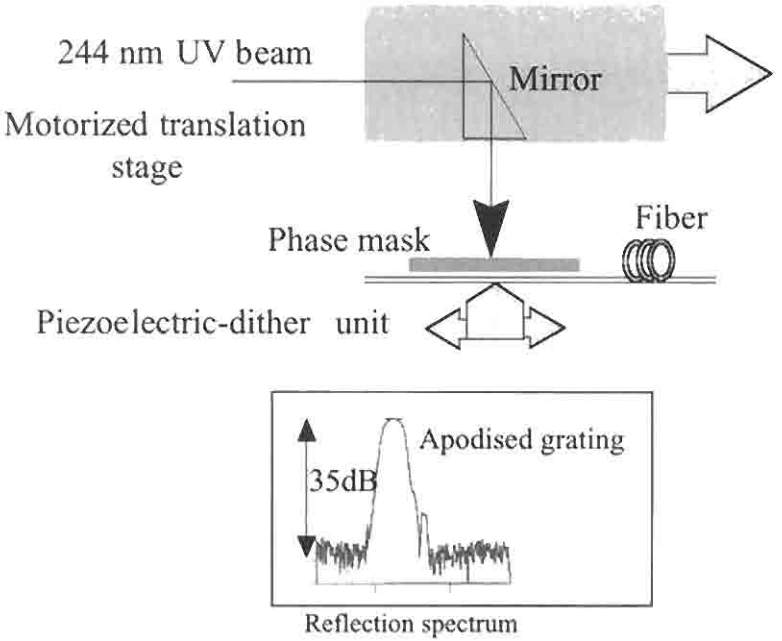

Figure 5.12: The moving phase mask/fiber method for apodizing gratings as well as inducing chirp. The lower inset shows the achieved reflection spectrum of an unchirped grating, with side lobes 35 dB below the peak (after Ref. [20]).

precision piezoelectric translator. Depending on the position of the UV beam, the fiber is dithered in the scanning direction backward and forward, to wash out the grating being inscribed by the required amount. Thus, if the dither amplitude is a linear function of position of the UV beam, with zero movement at the center of the phase mask, an apodized grating is written. Note that the smearing of the grating occurs over the entire length of the writing beam width, so it is essential that the spot size be kept small. The result of apodization is also shown in the inset in Fig. 5.12. The side lobes have been suppressed by approximately 13 dB below the side modes of a uniform period grating [20,21].

If the velocity of the fiber is v_f, the scanning UV beam moves at v_{sc} and the width of the beam is W, then the normalized amplitude of the refractive index modulation Δn varies as a sinc function:

$$\Delta n = \frac{\sin(\pi W v_f / \Lambda_g v_{sc})}{(\pi W v_f / \Lambda_g v_{sc})}. \tag{5.2.6}$$

From Eq. (5.2.6) it follows that the modulation index goes to zero for the |argument| = π radians, so that

$$v_f = \frac{\Lambda_g}{W} v_{sc}. \tag{5.2.7}$$

Equation (5.2.7) shows the obvious result that if the width of the beam is equal to the period, then $v_f = v_{sc}$ to wash out the refractive index modulation. In general, the beam width $W \gg 100 \times \Lambda_g$, so that the velocity of the fiber is $\ll 1\%$ of the scanning velocity.

The relative movement of the fiber with respect to the scanning beam changes the Bragg wavelength of the grating, which is easily calculated as

$$\frac{\Delta\Lambda}{\Lambda_g} = \frac{v_f}{v_{sc}}. \tag{5.2.8}$$

Combining Eqs. (5.2.7) and (5.2.8) directly leads to the chirp as a function of the width of the UV beam,

$$\frac{\Delta\Lambda}{\Lambda_g} = \frac{\Lambda_g}{W}. \tag{5.2.9}$$

Therefore, the maximum wavelength shift is inversely proportional to the width of the beam. This condition is similar to the one encountered in the MPF technique: The maximum is equivalent to the fiber moving one period during the time it takes the UV beam to move a distance equal to its width at the scanning velocity. Using Eq. (5.3.9) in Eq. (5.3.7), and recalling the relationship between the grating period and the Bragg wavelength, leads to

$$\Delta n = \frac{\sin(\Delta\beta W)}{(\Delta\beta W)}, \tag{5.2.10}$$

where

$$\Delta\beta = \frac{2\pi_{eff}}{\lambda_{Bragg}} \cdot \frac{\Delta\lambda}{\lambda_{Bragg}}$$

is the equivalent of "phase detuning" between the Bragg wavelength and the grating that is being written over the width of the beam. Note here that at constant fiber velocity (and scanning beam), the wavelength shifts; if the fiber velocity changes during the scan, the result is a chirped grating.

This is especially useful, since apodization and chirp can be programmed in at the same time. A parameter that needs to be attended to while fabricating a chirped grating is the loss in the amplitude of the refractive index modulation. This must be compensated for, since otherwise the grating will have a varying reflectivity as a function of wavelength. There are two possibilities. The first one is to slow down both v_f and v_{sc} while maintaining the ratio so that a stronger grating results as the grating is chirped. Alternatively, the intensity of the writing beam may be increased to take account of the reduction in the amplitude of the modulation index. There is no published data available on the choice of either approach [20].

It is useful to consider the application of this technique in the fabrication of longer, chirped apodized gratings. Very much in the spirit of the *sinc* profile TH reflection grating and the superstructure grating, another approach to the production of long chirped gratings uses a simple analogy in Fourier transforms. A grating with a uniform period, modulated by a low spatial frequency, pure sinusoidal envelope of period Λ_e, will produce two side bands only. This grating has the following refractive index amplitude modulation profile:

$$\Delta n(z) = 2n\Delta n_0 \cos\left(\frac{2\pi N}{\Lambda_g}\right) \cos\left(\frac{2\pi M}{\Lambda_e}\right), \tag{5.2.11}$$

where N and M are integers indicating the orders of the periods involved, and $2n\Delta n_0$ is the UV induced index change. Simplifying Eq. (5.2.11) directly leads to the resultant spatial frequencies,

$$\begin{aligned}\Delta n(z) = n\Delta n_0 \left\{ \cos\left(\frac{2\pi N}{\Lambda_g}\left[1 + \frac{M\Lambda_g}{N\Lambda_e}\right]z\right)\right. \\ \left. + \cos\left(\frac{2\pi N}{\Lambda_g}\left[1 - \frac{M\Lambda_g}{N\Lambda_e}\right]z\right)\right\}.\end{aligned} \tag{5.2.12}$$

There are only two spatial frequencies present, at the sum and difference frequencies. Note that in Eq. (5.2.12) the amplitude of the index modulation for each spatial frequency has been halved and that two Bragg reflections will occur. Note also that there can be higher order terms according to the ratio of N and M. The next reflection will occur at roughly half the fundamental Bragg wavelength, for $N = M = 2$, and at shorter wavelengths for other orders, predicted here but not as yet reported in the literature. The new reflections occur at a wavelength separation of

$$\Delta\lambda = \frac{\lambda_{Bragg}^2}{2n_{eff}\Lambda_e} \approx \lambda_{Bragg}\frac{\lambda_{Bragg}}{\lambda_e}. \tag{5.2.13}$$

In Eq. (5.2.13), the denominator is approximately the Bragg wavelength λ_e "phase matched" to the period of the *envelope*, so that the fractional change in the fundamental Bragg wavelength is the same as the ratio of the two wavelengths.

As in the case of the TH grating, a phase shift of π radians has to be introduced at each zero crossing, shown in Fig. 5.13. With a chirped grating, the bandwidth and the envelope period may be chosen so that the side bands are adjacent to each other. Ibsen *et al.* [22] demonstrated such a grating by incorporating a continuous chirp of 2.7 nm over a grating length of 1 meter, as well as an envelope period of 291 μm. Approximately 3500 individual periods were printed with as many π-phase stitches. The grating was apodized using a raised cosine envelope over 10% of the length of the grating on each edge. The reflection and delay spectrum is shown in Fig. 5.14. The dispersion of each section was reported to be 3.630 nsec/nm (short wavelength) and 3.607 nsec/nm (long wavelength), respectively, with a total delay of 9.672 ns. These gratings are designed to compensate the dispersion of 200 km of standard fiber with a dispersion of 17 ps/nm/km.

Typically, to produce side bands at 2 nm away from the Bragg matched wavelength, the period of the envelope will be in the region of 300–400 microns. This is roughly the period required to couple a guided mode to a copropagating radiation mode (long-period gratings, see Chapter 4), so that at some wavelength (not necessarily within the chirped bandwidth), it is predicted that strong radiation loss will be observed. The radiation loss will be due to the *stitches* and not the envelope, since for the latter

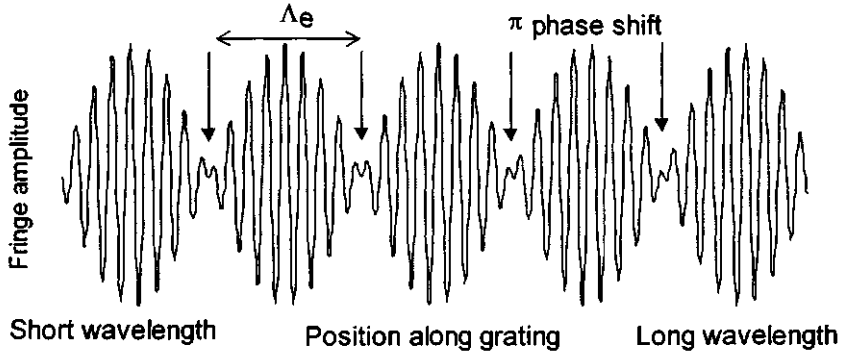

Figure 5.13: The modulated fringe profile of the moiré chirped grating with periodic π phase shifts.

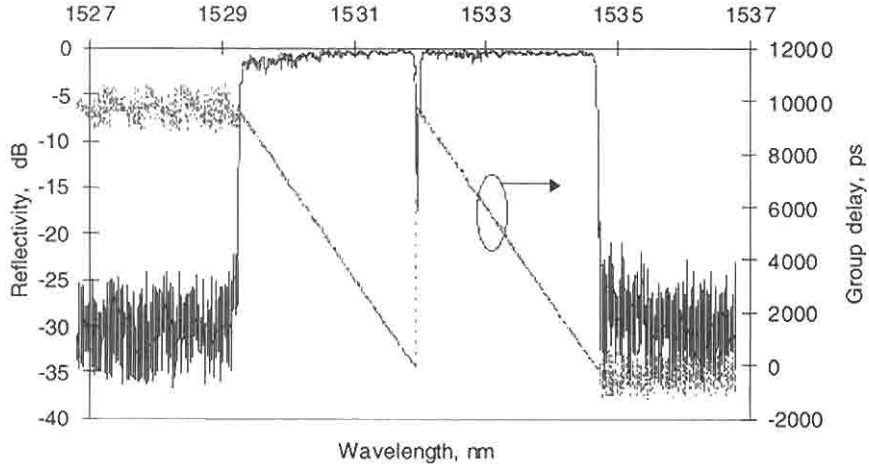

Figure 5.14: Reflectivity and delay characteristics of the chirped moiré grating (from: Ibsen M., Durkin Michael K., and Laming R. I., "Chirped Moiré gratings operating on two-wavelength channels for use as dual-channel dispersion compensators," *IEEE Photon. Technol. Lett.* **10**(1), 84–86, 1998.)

the average index remains unchanged. This prediction has not yet been confirmed. In order to avoid this problem, it is necessary to choose the bandwidth of the grating and the envelope period judiciously.

5.2.7 The symmetric stretch apodization method

The methods for apodization that are most flexible also require active management under the control of a computer. This inevitably means synchronization of the grating inscribing UV pulse and the position of the fiber (cf. MPF as well as the MPM methods). While the flexibility is desirable for a number of applications, simpler methods such as the apodized phase mask are intrinsically faster and probably better suited to mass production. However, as has been discussed, the apodized phase mask is fragile in its reported implementation and perhaps less predictable in fabrication. It also has the severe limitation of allowing an apodized grating that is only as long as the phase mask. This requires a selection of phase masks, unless a tunable interferometer is used; this, unfortunately, counters the argument for using the phase mask, since it defines the

wavelength for mass replication. Thus, a number of apodized phase masks may be required, each of a different wavelength and length.

Apodization requires that the refractive index modulation at the edges of the grating gradually disappear. As described in Section 5.2.1, a moiré grating is composed of two individual gratings, which leads to apodization. The Bragg wavelength of a grating can be changed by stretching the fiber prior to writing [23,24]. Therefore, two gratings written at the same location but differing in wavelength by exactly one period will be apodized. The problem is, how can the two gratings be overlaid such that they have the correct relative phase between them? One possibility is to use symmetric fiber stretching during the inscription of a grating [25]. This poor man's apodization technique — the symmetric stretch apodization method (SAM) — is not only simple to operate, but also applicable to *any* type of grating that needs to be apodized.

Figure 5.15 shows the schematic of the principle of inscription by symmetric stretching of the fiber. The technique can be understood as follows: A grating is first written into a fiber in its relaxed state (Fig 5.15b), for example, by scanning a phase mask, although the method of inscription is unimportant. The fiber is then stretched by straining it in opposite directions by exactly one period of the grating in the fiber, and another grating written on top of the first. Since the fiber is stretched, the inscribed grating is one period longer than the first (Fig. 5.15a) and also symmetrically overlaid (Fig. 5.15c).

The central part of the grating periods are overlaid in phase, while farther away from the center they become increasingly out of phase, until the edges, where they are π out of phase. The difficulty of ensuring that

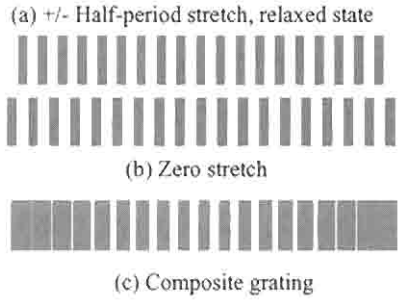

Figure 5.15: A schematic of the symmetric stretch scheme for apodizing gratings. See text for explanations.

both gratings receive the same UV dose is overcome by stretching the fiber back and forth continuously, e.g., by using two piezoelectric transducers, oscillating out of phase. If the fiber is periodically stretched at a high enough frequency, a perfectly apodized grating will result. The apodization function has a pure half-sinusoidal period as an envelope.

For a scanning phase mask interferometer, it is necessary to ensure that the scan speed is such that each point of the fiber is exposed to the UV beam for at least a single stretching cycle, for each scan. This is easily achieved by adjusting the scan speed to be slow enough, depending on the frequency of the stretcher. For a given UV beam width, W_{UV}, and scan speed, V_{UV} m/sec, the frequency f of the stretching oscillator is

$$f = \frac{V_{UV}}{W_{UV}}. \tag{5.2.14}$$

Apodization works for a variety of situations: If the UV beam is static, the stretching scheme frequency is really not that important, so long as the UV power is low enough to enable the grating to form in a time frame much greater than a single period of the oscillator frequency. This condition is generally met unless the grating is written in a single shot from a pulsed laser. A certain amount of care does need to be taken if the apodization is to be performed with a pulsed laser source. It is important that the grating be inscribed over many pulses so that pulse averaging takes place, as well as than every possible position of the stretch of the fiber be inscribed with a grating. One exception is if the grating is inscribed in two uniform pulses of identical intensity, one for each extreme position of the stretch.

Apodization of the grating is *continuous* and not stepped, since each part of the fiber is stretched exactly the correct amount for apodization. This is not true of the MPM technique, in which a whole subgrating length is "smeared" out by the same amount, so that only quasi-continuous apodization is possible. The same applies to the MPF technique. The reason both techniques work is because some of the index change is sacrificed over the finite length of the subgrating. In the case of the MPF scheme, each subgrating tries to print the new grating on what was printed before, but slightly altered. In the MPM, it continuously builds on the regions that have been "wrongly" printed, the result of a finite length of subgrating. There is normally enough refractive index change available for this limitation not to be a problem.

The apodization scheme is independent of the length of the grating, the only requirement being that the fiber be stretched by half-a-period in each direction, so that for a chirped grating, one end of the fiber is stretched slightly more than the other, by adjusting the stretch on that side. For uniform period gratings, no adjustment is necessary when changing the wavelength of the phase mask in the same spectral window (e.g., 1500 nm). Figure 5.16 shows the experimental setup of the equipment used in SAM.

The required stretch to form perfectly apodized gratings as a function of length is shown in Fig. 5.17. Even for relatively short gratings, the strain is easily applied. Another possibility with this method is to write two gratings under static strain to form moiré gratings.

By switching off one stretcher, the grating will be apodized only on the stretched side. As a result, left- and right-hand-end apodization may be performed independently. For super-step-chirped gratings [26], this feature allows apodization of each end of the grating. For the first, shortest-wavelength grating, the short-wavelength end is apodized; other intermediate gratings are printed sequentially without apodization, except for the last, longest-wavelength grating, in which the right-hand, long-wavelength end is apodized by switching on the RH piezoelectric stretcher.

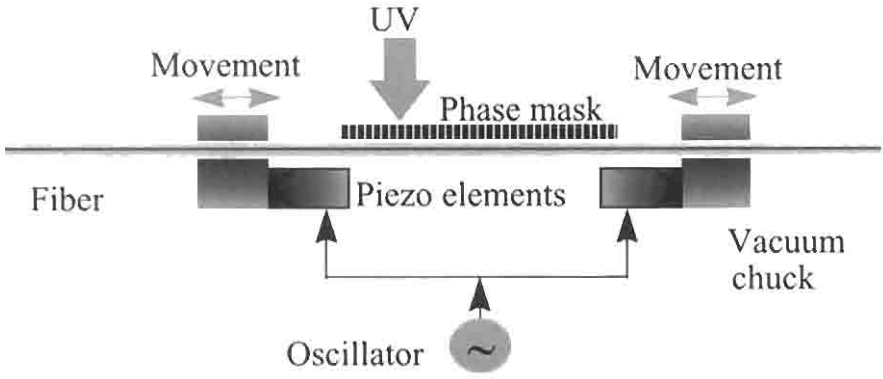

Figure 5.16: The symmetric stretching apodization method (SAM). The phase mask may be replaced by any interferometer. The displacement of the piezoelectric stretchers is monitored by position sensors to set the required stretch [25].

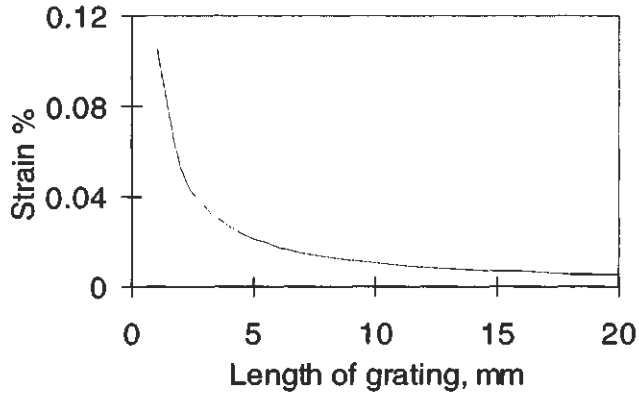

Figure 5.17: The strain applied to a fiber for perfect apodization as a function of grating length for the SAM technique.

A schematic of this principle of making ultralong gratings is shown in Fig. 5.18.

With greater stretch of the fiber, a larger number of cycles of the apodization profile may be written, for example, a *bowtie* profile. Turning off both stretchers may alter the apodization profile after a single pass. The next over laid grating is left unapodized, thereby building a modified cosine refractive index modulation profile.

Increasing the stretch further forms a single cosine envelope, shown in Fig. 5.19. The stretch method has the same effect as the dual frequency moiré grating apodization. At the zero crossing of the envelope, a π phase

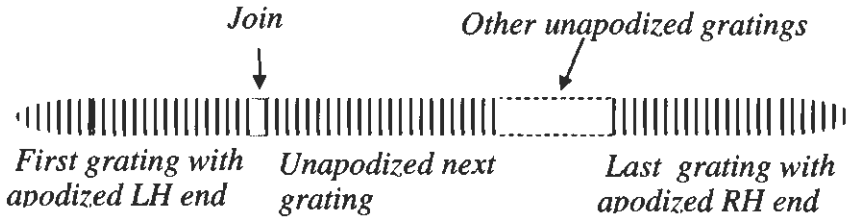

Figure 5.18: The super-step chirped grating, apodized on each end. With a uniform period phase mask, the chirp is zero so that a long, unchirped apodized grating can be written. Careful alignment can eliminate the stitch error at the join, or it may be UV "trimmed" [26].

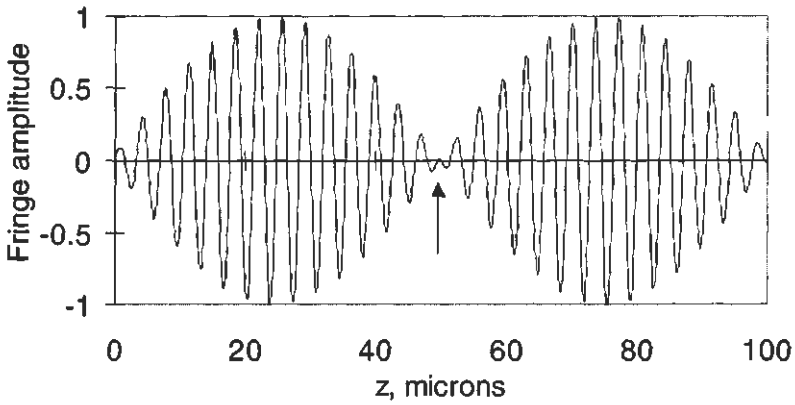

Figure 5.19: A single-period cosine envelope moiré grating formed by stretching the fiber by twice the required amount for perfect apodization (as in Fig. 5.15). The arrow indicates the position of the *automatically* introduced π phase shift in the fringes, equivalent to a $\pi/2$ phase shift at the Bragg wavelength. The length of the grating has been chosen to be deliberately short to show the occurrence of the phase shift.

change occurs between the two sections of the fringes, as can be seen in Fig. 5.19. This effect can be used to automatically introduce multiple, regularly spaced $\pi/2$ phase shifts at the Bragg wavelength for the fabrication of a top-hat reflection spectrum and multiple band-pass filters (also see Section 5.2.6). The difference between stretching or the dual-frequency multiple-period moiré gratings and the MPF technique for writing a similar grating is that in the latter, a deliberate phase shift has to be written in, whereas in the former, the phase shift is *automatically* introduced.

5.3 Fabrication requirements for apodization and chirp

As has been demonstrated in Section 5.2.6, the maximum chirp that can be written using the two mini-grating replication methods (MPF and MPM) is dependent on the length of the subgrating; in the case of the 1-mm-long subgrating for the MPF method, it is only possible to write a grating with a chirp of ~1 nm, since it is equivalent to a change of one period in 1 mm. In order to write larger chirps and apodize the grating

at the same time, a smaller subgrating must be written. The maximum chirp that can be produced from a subgrating length of δL_g is

$$\Delta\lambda = 2n_{eff}\frac{\Lambda_g}{\delta L_g}. \tag{5.3.1}$$

A grating with a bandwidth of 10 nm near the Bragg wavelength of ~1.55 μm requires a subgrating length of ~300 μm. The second point to remember is that the refractive index modulation remains almost unchanged with the chirp induced using the MPF scheme, which can only be used with a pulsed laser. A reduction in the refractive index modulation occurs when a chirp is induced with the MPM method. It can be compensated for to some extent by adjusting the irradiation intensity or by changing the movement velocities of the fiber or phase mask and UV beam, but it requires a CW writing beam. Both methods allow the inscription of long gratings but do require a movement stage with a translation capability at least as long as the grating to be written.

The complication of saturation effects [27,28] has not been addressed in the case of strong gratings written using either of these methods, although certain fibers show a linear response to the time of exposure to UV radiation at a longer wavelength of 334 nm and a much increased writing time [29]. Undoubtedly these will play an important role as the requirements for the types of gratings become more demanding. The effect of linearity of the photosensitive response of the fiber to, for example, the change in the local intensity is as yet unknown. The further, more serious issue of the out-diffusion of hydrogen/deuterium from long gratings has also not been discussed. Out-diffusion causes a reduction in the refractive index of both the UV-exposed and the unexposed regions [30,31]. A differential change in the refractive index between the two regions will lead to a degradation in the transfer characteristics of long gratings, since the phase change accumulates over its entire length.

Both the MPF and MPM methods are flexible and capable of apodizing gratings with arbitrary refractive index modulation profiles and are capable of the production of identical grating characteristics.

The issues related to the other schemes, such as the apodized phase mask, although convenient, are limited flexibility allowing only the replication of the type of apodization programmed in the phase mask. There is a restriction on the maximum size of the phase mask as well as on the reproducibility of the apodized phase mask. Although, as with the step-chirped phase mask [6], it is possible to combine apodization and chirp

in a phase mask. However, the symmetric stretch apodization method combines the two and is flexibly applied to any length of grating. SAM is excellent for long gratings, since the stretch is fixed by the period of the grating, and therefore the strain changes inversely with length. This is shown in Fig. 5.17. For a 1-mm grating, the fiber has to be strained by ~0.1%, which is acceptable, but drops to an insignificant 0.01% for a 10-mm grating. It is, however, very important to ensure that the stretch *is* symmetric; otherwise, the apodization will not be satisfactory. Once the interferometer is aligned, then any length of grating may be apodized. If the grating is not symmetrically placed between the stretchers, then the piezoelectric movement can be adjusted to stretch one end of the fiber more than the other, easily compensating for the misalignment. Finally, certain types of fiber show a photosensitivity that is a function of applied strain [27]. However, the strain used for the apodization of fibers is only a small fraction of that reported in Ref. [27] and should not pose a problem for gratings longer than a millimeter. For long moiré grating formation, the applied strain will also remain low enough to not to cause nonlinearity in the photosensitivity.

References

1 "Caecilla," *Encyclopedia Britannica, Micropaedia*, Vol. 2, p. 715.

2 Hill K. O., "Aperiodic distributed-parameter waveguides for integrated optics," *Appl. Opt.* **13**, 1853–1856 (1974).

3 Matsuhara M. and Hill K. O., "Optical-waveguide band-rejection filters: design," *Appl. Opt.* **13**, 2886–2888 (1974).

4 Mizrahi V. and Sipe J. E., "Optical properties of photosensitive fiber phase gratings," *J Lightwave Technol.* **11**(10), 1513–1517 (1993).

5 Meltz G., Morey W. W., and Glenn W. H., "Formation of Bragg gratings in optical fibres by transverse holographic method," *Opt. Lett.* **14**(15), 823 (1989).

6 Kashyap R., McKee P. F., and Armes D., "UV written reflection grating structures in photosensitive optical fibres using phase-shifted phase-masks," *Electron. Lett.* **30**(23), 1977–1978 (1994).

7 Pakulski G., Moore R., Maritan C., Shepard F., Fallahi M., Templeton I., and Champion G., "Fused silica masks for printing uniform and phase adjusted gratings for distributed feedback lasers," *Appl. Phys. Lett.* **62**(3), 222 (1993).

8 See, for example, Morgan D. P., "Surface-Wave Devices for Signal Processing." Elsevier, Oxford (1985).

9 Froehlich H.-G. and Kashyap R., "Two methods of apodisation of fibre Bragg gratings," *Opt. Commun., 157*(6), 273–281 (1998).

10 Malo B., Thériault S., Johnson D. C., Bilodeau F., Albert J., and Hill K. O., "Apodised in-fibre Bragg grating reflectors photoimprinted using a phase mask," *Electron. Lett.* **31**(3), 223–225 (1995).

11 Dyer P. E., Farley R. J., Giedl R., Byron K. C., and Reid D., "High reflectivity fibre gratings produced by incubated damage using a 193 nm ArF laser," *Electron. Lett.* **30**(11), 860–862 (1994).

12 Albert J., Hill K. O., Malo B., Théirault S., Bilodeau B., Johnson D. C., and Erikson L. E., "Apodisation of spectral response of fibre Bragg gratings using a phase mask with a variable diffraction efficiency," *Electron. Lett.* **31**(3), 222–223 (1995).

13 Kashyap R., McKee P. F., Campbell R. J., and Williams D. L., "A novel method of producing photo-induced chirped Bragg gratings in optical fibres," *Electron. Lett.* **30**(12), 996–997 (1994).

14 Albert J., Thériault S., Bilodeau F., Johnson D. C., Hill K. O., Sixt P., and Rooks M. J., "Minimisation of phase errors in long fiber Bragg grating phase masks made using electron beam lithography," *IEEE Photon. Technol. Lett.* **8**(10), 1334–1336 (1996).

15 Albert J., Hill K. O., Johnson D. C., Bilodeau F., and Rooks M. J., "Moiré phase masks for automatic pure apodisation of fibre Bragg gratings," *Electron. Lett.* **32**(24), 2260–2261 (1996).

16 Stubbe R., Sahlgren B., Sandgren S., and Asseh A., "Novel technique for writing long superstructured fiber Bragg gratings," in *Photosensitivity and Quadratic Nonlinearity in Glass Waveguides: Fundamentals and Applications*, Vol. 22, 1995 OSA Technical Series (Optical Society of America, Washington DC, 1995), pp. PD1-(1–3) (1995).

17 Storøy H., "Fibre Bragg gratings and fibre optic structural strain sensing," Ph.D. Thesis, Norwegian University of Science and Technology, NTUT (1997).

18 Storøy H., Engan H. E., Sahlgren B., and Stubbe R., "Position weighting of fiber Bragg gratings for bandpass filtering," *Opt. Lett.* **22**(11), 784–786 (1997).

19 Kino G. S., *Acoustic waves: Devices, Imaging, and Analog Signal Processing*. Prentice Hall, New Jersey (1987).

20 Cole M. J., Loh W. H., Laming R. I., Zervas M. N., and Barcelos S., "Moving fibre/phase mask-scanning beam technique for enhanced flexibility in producing fibre gratings with a uniform phase mask," *Electron. Lett.* **31**(17), 92–94 (1995).

21 Cole M. J., Loh W. H., Laming R. I., Zervas M. N., and Barcelos S., "Moving fibre/phase mask-scanning beam technique for writing arbitrary profile fibre gratings with a uniform phase mask," in *Photosensitivity and Quadratic Nonlinearity in Glass Waveguides: Fundamentals and Applications*, Vol. 22, 1995 OSA Technical Series (Optical Society of America, Washington DC, 1995), pp. PD1-(1–3) (1995).

22 Ibsen M., Durkin Michael K., and Lamming R. I., "Chirped Moiré gratings operating on two-wavelength channels for use as dual-channel dispersion compensators," *IEEE Photon. Technol. Lett.* **10**(1), 84–86 (1998).

23 Campbell R. J. and Kashyap R., "Spectral profile and multiplexing of Bragg gratings in photosensitive fibre," *Opt. Lett.* **16**(12), 898–900 (1991).

24 Byron K. C., Sugden K., Bircheno T., and Bennion I., "Fabrication of chirped Bragg gratings in photosensitive fibre," *Electron. Lett.* **29**(18), 1659 (1993).

25 Kashyap R., Swanton A., and Armes D. J., "A simple technique for apodising chirped and unchirped fibre Bragg gratings," *Electron. Lett.* **32**(14), 1226–1228 (1996).

26 Kashyap R., Froehlich H.-G., Swanton A., and Armes D. J., "1.3 m long superstep chirped fibre Bragg grating with a continuous delay of 13.5 ns and bandwidth 10 nm for broadband dispersion compensation," *Electron. Lett.* **32**(19), 1807–1809 (1996).

27 Niay P., Bernage P., Douay M., Taunay T., Xie W. X., Martinelli G., Bayon J. F., Poignant H., and Delevaque E., "Bragg grating photoinscription within various types of fibers and glasses," in *Photosensitivity and Quadratic Nonlinearity in Glass Waveguides: Fundamentals and Applications*, Vol. 22, 1995 OSA Technical Series (Optical Society of America, Washington, DC, 1995), paper SUA1, pp. 66–69 (1995).

28 Douay M., Xie W. X., Taunay T., Bernage P., Niay P., Cordier P., Poumellec B., Dong L., Bayon J. F., Poignant H., and Delevaque E., "Densification involved in the UV-based photosensitivity of silica glasses and optical fibers," *IEEE J. Lightwave. Technol.* **15**(8), 1329–1342 (1997).

29 Grubsky V., Starburodov D. S. and Feinberg J., "Wide range and linearity near-UV induced index change in hydrogen-loaded fibers: Applications for Bragg grating fabrication," in *Bragg Gratings, Photosensitivity, and Poling in Glass Fibers and Waveguides: Applications and Fundamentals*, Vol. 17, OSA Technical Digest Series (Optical Society of America, Washington, DC, 1997), Paper BME3, pp. 156–158.

30 Malo B., Albert J., Hill K. O., Bilodeau F., and Johnson D. C., "Effective index drift from molecular hydrogen diffusion in hydrogen-loaded optical fibres and its effect on Bragg grating fabrication," *Electron. Lett* **30**(5), 442–444 (1994).

31 Bhakti F., Larrey J., Sansonetti P., and Poumellec B., "Impact of hydrogen in-fiber and out-fiber diffusion on central wavelength of UV-written long period gratings," in *Bragg Gratings, Photosensitivity, and Poling in Glass Fibers and Waveguides: Applications and Fundamentals*, Vol. 17, OSA Technical Digest Series (Optical Society of America, Washington, DC, 1997), paperBSuD4, pp. 55–57.